Journal of Basic and Environmental Sciences 2 (2015) 36 – 51 ISSN 2356-6388

Novel inhibitors for carbon steel pipelines corrosion during acidizing of oil and gas wells

M.A. Hegazy[a,*], A.Y. El-Etre[b], K. M. Berry[b]

[a] Egyptian Petroleum Research Institute (EPRI), Nasr City, Cairo, Egypt
[b] Chemistry Dept., Faculty of Science, Benha University, Benha, Egypt

[*] Corresponding author. Tel.: +20 1002653529; fax: +20 222747433.
E-mail address: mohamed_hgazy@yahoo.com (M.A. Hegazy).

Article Information

Received; 12 May. 2014
In Revised form; 28 May 2014
Accepted; 28 May 2014

Keywords:
Steel
Weight loss
Polarization
EIS
Acid inhibition.

Abstract

The inhibition effect of three novel Schiff bases on corrosion of carbon steel was studied in 1 M HCl solution. The inhibition efficiency was measured by weight loss, potentiodynamic polarization and electrochemical impedance spectroscopy (EIS) methods. The obtained results showed that the prepared Schiff bases are very good corrosion inhibitors. The adsorption of inhibitors on carbon steel surface obeys Longmuir adsorption isotherm. The adsorption of these Schiff bases involves two types of interaction physical and chemical adsorption. The inhibition efficiency increases with increasing inhibitor concentration and temperature. Quantum chemistry calculations for the geometrical full optimization of the inhibitors were calculated.

1. Introduction

Acidizing process involves the injection of chemicals to eat away at any skin damage, "cleaning up" the formation, thereby improving the flow of reservoir fluids. A strong acid (usually HCl) is used to dissolve rock formations. Acid can also be used to clean the wellbore of some scales that form from mineral laden produced water. The pickling of mild steel in acid solution is an important processing step to remove the oxide formed during annealing and hot rolling [1,2]. During the pickling process it is necessary to remove the segregated oxide however a more extensive attack is undesirable so it is very important to use corrosion inhibitors [3,4].

Iron and its alloys, which are widely used in a lot of industrial processes, corrode causing considerable costs. Many materials were studied to decrease the corrosion rate. The use of corrosion inhibitors is one of the most practical methods for protection against corrosion in acidic media. Most well-known acid inhibitors are organic compounds such as those contain hetero atom; oxygen, nitrogen and sulfur as well as aromatic ring [5-14]. The measurement of corrosion rate as a function of the inhibitor concentration in the aggressive electrolyte is the conventional method of the characterizing the inhibitor system. The efficiency of inhibition basically depends on the structure of the inhibitor molecule, specific interaction between function groups and the metal surface and the hetero atoms that play an important role in the inhibition mechanism due to the free electron pairs they possessed [15-17].

The aim of this work is to determine the inhibition efficiency of (Z)-N-(1-methylpyrrolidin-2-ylidene)-2-phenylethanamine (Schiff base A), 2-((1-methylpyrrolidin-2-ylidene) amino) ethanol (Schiff base B) and (E)-4-((1-methylpyrrolidin-2-ylidene)amino)phenol (Schiff base C) as novel inhibitors for the corrosion of carbon steel in 1 M HCl solution. The inhibition efficiency was determined using weight loss technique, potentiodynamic polarization and electrochemical impedance spectroscopy. The thermodynamic parameters were calculated for interpretation of inhibition mechanism of the synthesized Schiff bases. Some quantum parameters were calculated to elucidation experimental results.

2. Material and experimental methods

2.1. Carbon steel

Tests were performed on carbon steel coupons were obtained from the pipelines used in petroleum production. It has the following composition: 0.11% C, 0.45% Mn, 0.04% P, 0.05% S, 0.25% Si, and the reminders Fe.

2.2. Synthesis of novel Schiff bases

Reflux one mole of 1-methylpyrrolidin-2-one with one mole of 2-phenylethanamine, 2-aminoethanol and 4-aminophenol in 100 ml ethanol as solvent in 250 ml round flask at 70 ºC for 24 h. This mixture was allowed to cool down, and the obtained materials were further purified by diethyl ether then recrystallized by ethanol to produce (Z)-N-(1-methylpyrrolidin-2-ylidene)-2-phenylethanamine, 2-((1-methylpyrrolidin-2 ylidene)amino)ethanol and (E)-4-((1-methylpyrrolidin-2-ylidene)amino) phenol respectively. The final products were dried under vacuum. The chemical structures of the synthesized Schiff bases are shown in Fig. 1. The chemical structure of the synthesized compounds was confirmed by ^{1}HNMR and Mass spectroscopy.

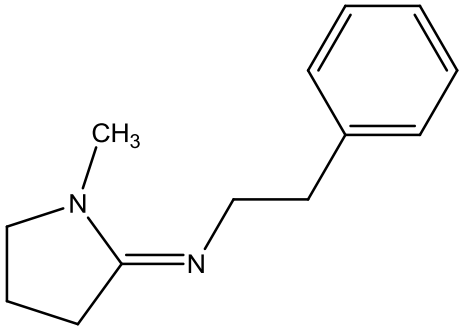

Schiff base A: (Z)-N-(1-methylpyrrolidin-2-ylidene)-2-phenylethanamine

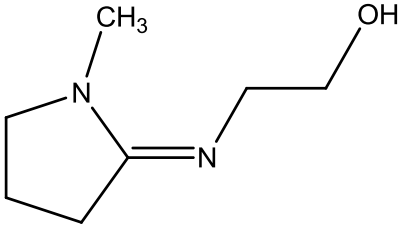

Schiff base B: 2-((1-methylpyrrolidin-2 ylidene)amino)ethanol

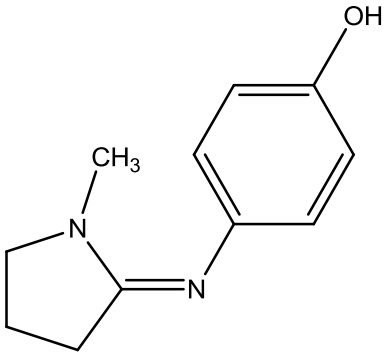

Schiff base C: (E)-4-((1-methylpyrrolidin-2-ylidene)amino) phenol

Fig. 1: The chemical structure of the synthesized Schiff bases.

2.3. Solution

The aggressive solution of 1 M HCl was prepared by dilution of the analytical grade 37 % HCl by distilled water. The concentration of the synthesized novel inhibitors was varied from $1x10^{-4}$ to $1x10^{-2}$ M for corrosion measurements.

2.4. Weight loss technique

The tested specimens were cut into 3cm x 6cm x 0.4cm and abraded with a series of emery paper (grade 320-400-600-800-1000-1200), cleaned successively with distilled water, ethanol and acetone and finally dried by dry air before use [18]. The samples were allowed to stand for 24 h in 1 M HCl solution in the absence and presence of different

concentrations of the inhibitors. Triplicate specimens were exposed for each experiment and the mean weight losses were reported.

2.5. Electrochemical techniques

Electrochemical experiments were carried out using a Voltalab 40 Potentiostat PGZ 301 in a conventional electrolytic cell with three-electrode arrangement: saturated calomel reference electrode (SCE), platinum rod as a counter electrode and the carbon steel rod as working electrode (WE). The electrode potential was allowed to stabilize for 30 minutes before starting the measurements. The exposed electrode area to the corrosive solution is 0.34 cm^2. The exposure surface was abraded with different grades of emery paper, degreased with acetone, washed with bidistilled water, and finally dried. The experiments were carried out at constant temperature (within ±1 °C). All experiments were conducted at 20 ºC. Potentiodynamic polarization curves were obtained by changing the electrode potential automatically (from -800 to -300 mV vs. SCE) at open circuit potential with scan rate of 2 mV s^{-1}. EIS measurements were carried out in a frequency range of 100 kHz to 30 mHz with amplitude of 5 mV peak-to-peak using ac signals at open circuit potential.

2.6. Quantum technique

Quantum chemistry calculations for the geometrical full optimization of the synthesized inhibitors were carried out at the DFT B3LYP/6-31++G(d,p) level using a Gaussian program package [19]. The following quantum chemical indices were considered: the energy of the highest occupied molecular orbital (E_{HOMO}), the energy of the lowest unoccupied molecular orbital (E_{LUMO}), Energy gab (ΔE), the dipole moment (μ), electronegativity (X), hardness (γ), softness (δ), chemical potential (π), molecular volume (M_g) and number of electron transfer (ΔN).

3. Results and discussion

3.1. Structure confirmation of the synthesized inhibitor

3.1.1. ^{1}HNMR spectroscopy

^{1}HNMR (DMSO - d6) spectrum of Schiff base (A) showed that δ, ppm at: δ=1.237–1.285 ppm (t, 2H, NC**H**$_2$CH$_2$Ar); δ=1.898–1.948 ppm (m, 2H, CH$_3$NCH$_2$C**H**$_2$CH$_2$); δ=2.149–2.203 ppm (t, 2H, NCH$_2$C**H**$_2$Ar); δ=2.494–2.506 ppm (t, 2H, C**H**$_2$CH$_2$CH$_2$NCH$_3$); δ=2.696 ppm (s, 3H, NC**H**$_3$); δ=3.277–3.324 ppm (t, 2H, CH$_3$NC**H**$_2$CH$_2$CH$_2$); δ=7.185–7.348 ppm (m, 5H, **Ar**-CH$_2$)

^{1}HNMR (DMSO - d6) spectrum of Schiff base (B) showed that δ, ppm at: δ=1.832–1.933 ppm (m, 2H, CH$_3$NCH$_2$C**H**$_2$CH$_2$); δ=2.144–2.199 ppm (t, 2H, CH$_2$CH$_2$C**H**$_2$C=N); δ=2.677 ppm (s, 3H, NC**H**$_3$); δ=3.270–3.317 ppm (t, 2H, CH$_3$NC**H**$_2$CH$_2$CH$_2$); δ=3.408–3.433 ppm (t, 3H, C=NC**H**$_2$CH$_2$O**H**); δ=4.237–4.359 ppm (t, 2H, C=NCH$_2$C**H**$_2$OH).

^{1}HNMR (DMSO - d6) spectrum of Schiff base (C) showed that δ, ppm at: δ=1.815–1.889 ppm (m, 2H, CH$_3$NCH$_2$C**H**$_2$CH$_2$C); δ=2.163–2.217 ppm (t, 2H, CH$_3$NCH$_2$CH$_2$C**H**$_2$C); δ=2.691 ppm (s, 3H, N-C**H**$_3$); δ=3.237–3.284 ppm (t, 2H, CH$_3$NC**H**$_2$CH$_2$CH$_2$C); δ=4.719 ppm (s, 1H, Ar-O**H**); δ=6.012–6.047 ppm (m, 2H, o-phenolic neucleous, δ=6.776–6.805 ppm (m, 2H, m-phenolic neucleous). ^{1}HNMR spectrum of Schiff base (C) is illustrated in Fig. 2.

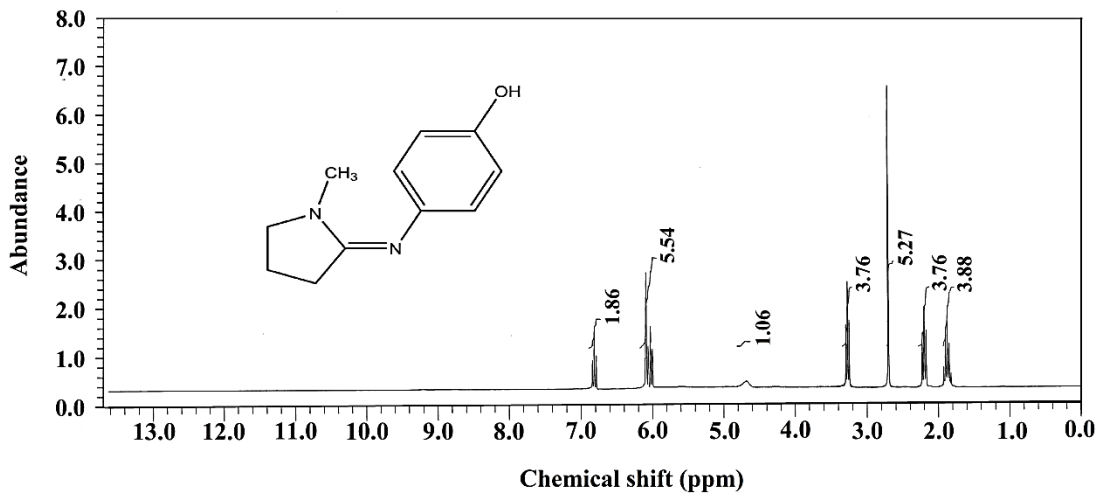

Fig. 2: ^{1}H NMR spectrum of Schiff base (C).

3.1.2. Mass spectroscopy

The mass spectrum of Schiff base (A) showed that the molecular ion peak and base peak m/z 202 (100%) $C_{13}H_{18}N_2$, 56 (18.36%) C_3H_6N, 68 (35.81%) C_4H_6N, 77 (36.31%) C_6H_5, 83 (39.33%) C_5H_9N, 91 (45.50%) C_7H_7, 97 (46.31%) $C_5H_9N_2$, 111 (50.08%) $C_6H_{11}N_2$, 112 (17.03%) $C_6H_{12}N_2$, 187 (33.92%) $C_{12}H_{15}N_2$.
The mass spectrum of Schiff base (B) showed that the molecular ion peak and base peak m/z 142 (100%) $C_7H_{14}N_2O$, 59 (42.22%) C_2H_5NO, 68 (33.41%) C_4H_6N, 82 (26.81%) $C_4H_6N_2$, 83 (47.54%) C_5H_9N, 97 (50.41%) $C_5H_9N_2$, 111 (33.22%) $C_6H_{11}N_2$, 125 (44.33%) $C_7H_{13}N_2$, 127 (29.3%) $C_6H_{11}N_2O$.
The mass spectrum of Schiff base (C) showed that the molecular ion peak and base peak m/z 190 (100%) $C_{11}H_{14}N_2O$, 68 (27.81%) C_4H_6N, 76 (70.33%) C_6H_4, 82 (27.66%) $C_4H_6N_2$, 83 (26.82%) C_5H_9N, 86 (23.94%) C_5H_9N, 90 (36.42%) C_6H_4N, 93 (46.81%) C_6H_5O, 97 (38.86%) $C_5H_9N_2$, 107 (28.66%) C_6H_5NO, 119 (29.64%) C_7H_5NO, 148 (21.11%) $C_8H_8N_2O$, 173 (24.36%) $C_{11}H_{13}N_2$, 175 (35.81%) $C_{10}H_{11}N_2O$.Mass spectrum of Schiff base (C) is illustrated in Fig. 3.

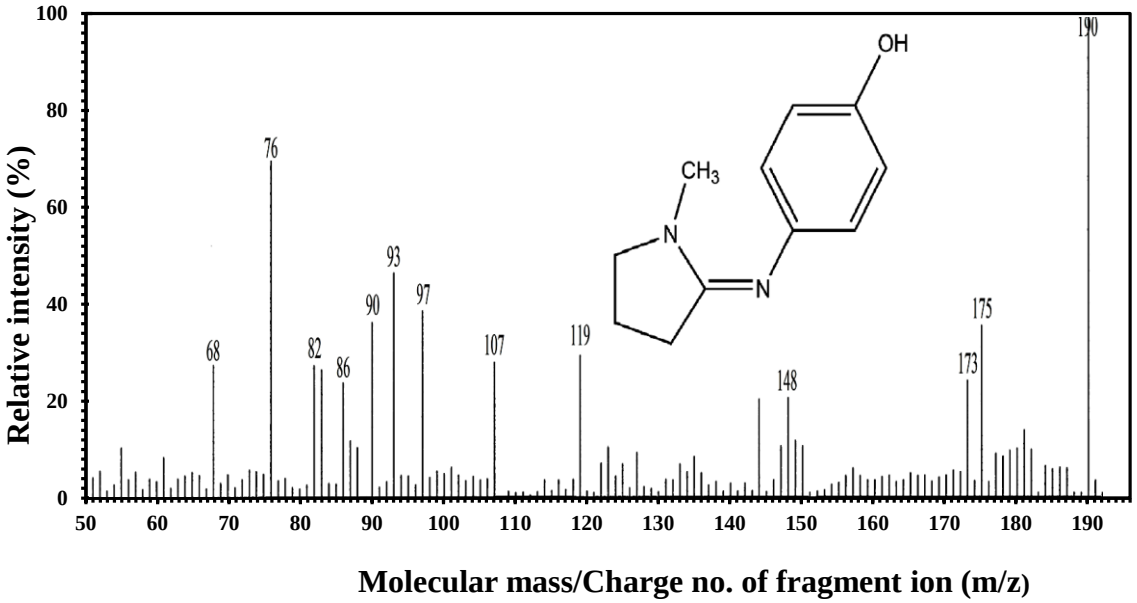

Fig. 3: Mass spectrum of Schiff base (C).

3.2. Weight loss measurements

The corrosion rate (k) is calculated from the following equation [20–22]:

$$k = \frac{W}{St} \qquad (1)$$

where W is the average weight loss, in mg, of three parallel carbon steel sheets, S, in cm^2, is the total area of the specimen and t, in h, is the immersion time. The inhibition efficiencies (η_w) of the prepared Schiff bases on the corrosion of carbon steel are calculated from the following equation [18, 20–22]:

$$\eta_w = \left(\frac{W_o - W}{W_o}\right) \times 100 \qquad (2)$$

where W_o and W are values of the weight loss without and with addition of the inhibitor, respectively.
The results of weight loss technique are represented in Table 1 and Fig. 4. Inspection of the data of Table 1 as well as Fig. 4 reveals that the three used compounds act as very good inhibitor for corrosion of carbon steel in the acidic medium. The inhibition efficiency increases with increasing of both inhibitor concentration and temperature. The inhibitive action of the used compound could be a result of adsorption of their molecules on the metal surface. Increasing inhibitor concentration increases the surface area covered by the adsorbed molecules leading to increasing the inhibition efficiency. Furthermore, the increase of inhibition efficiency with increasing temperature indicates that temperature favors and supports the adsorption process. This behavior suggests a chemosorption process through forming coordinat bonds between the lone pairs of electrons on the N and O atoms of the inhibitor molecules and vacant *d*-orbitals of the iron.

Table 1: Weight loss data for carbon steel 1 M HCl in the absence and presence of different concentrations of the synthesized Schiff bases at various temperatures

	Inhibitor conc. (M)	20 °C			35 °C			50 °C			65 °C		
		k mg cm^{-2} h^{-1}	Θ	η_w %	k mg cm^{-2} h^{-1}	Θ	η_w %	k mg cm^{-2} h^{-1}	Θ	η_w %	k mg cm^{-2} h^{-1}	Θ	η_w %
	0.00	0.5112	-	-	1.2730	-	-	2.9098	-	-	5.9036	-	-
A	$1x10^{-4}$	0.4385	0.14	14.2	1.0321	0.19	18.9	2.2245	0.24	23.5	4.4781	0.24	24.1
	$5x10^{-4}$	0.3377	0.34	33.9	0.7856	0.38	38.3	1.6902	0.42	41.9	3.3967	0.42	42.5
	$1x10^{-3}$	0.1802	0.65	64.8	0.4184	0.67	67.1	0.8984	0.69	69.1	1.8055	0.69	69.4
	$5x10^{-3}$	0.0571	0.89	88.8	0.1322	0.90	89.6	0.2832	0.90	90.3	0.5709	0.90	90.3
	$1x10^{-2}$	0.0418	0.92	91.8	0.0967	0.92	92.4	0.2066	0.93	92.9	0.4128	0.93	93.0
B	$1x10^{-4}$	0.4621	0.10	9.6	1.0513	0.17	17.4	2.2469	0.23	22.8	4.4587	0.24	24.5
	$5x10^{-4}$	0.3649	0.29	28.6	0.8191	0.36	35.7	1.7055	0.41	41.4	3.3272	0.44	43.6
	$1x10^{-3}$	0.2562	0.50	49.9	0.5879	0.54	53.8	1.2484	0.57	57.1	2.4798	0.58	58.0
	$5x10^{-3}$	0.1455	0.72	71.5	0.3356	0.74	73.6	0.7168	0.75	75.4	1.4308	0.76	75.8
	$1x10^{-2}$	0.0641	0.87	87.5	0.1481	0.88	88.4	0.3164	0.89	89.1	0.6269	0.89	89.4
C	$1x10^{-4}$	0.3407	0.33	33.3	0.7983	0.37	37.3	1.7282	0.41	40.6	3.0212	0.49	48.82
	$5x10^{-4}$	0.2712	0.47	46.9	0.6212	0.51	51.2	1.3173	0.55	54.7	2.4719	0.58	58.13
	$1x10^{-3}$	0.1981	0.61	61.2	0.4549	0.64	64.3	0.9669	0.67	66.8	1.9221	0.67	67.4
	$5x10^{-3}$	0.0775	0.85	84.8	0.1771	0.86	86.1	0.3747	0.87	87.1	0.7420	0.87	87.4
	$1x10^{-2}$	0.0398	0.92	92.2	0.0909	0.93	92.9	0.1921	0.93	93.4	0.3800	0.94	93.6

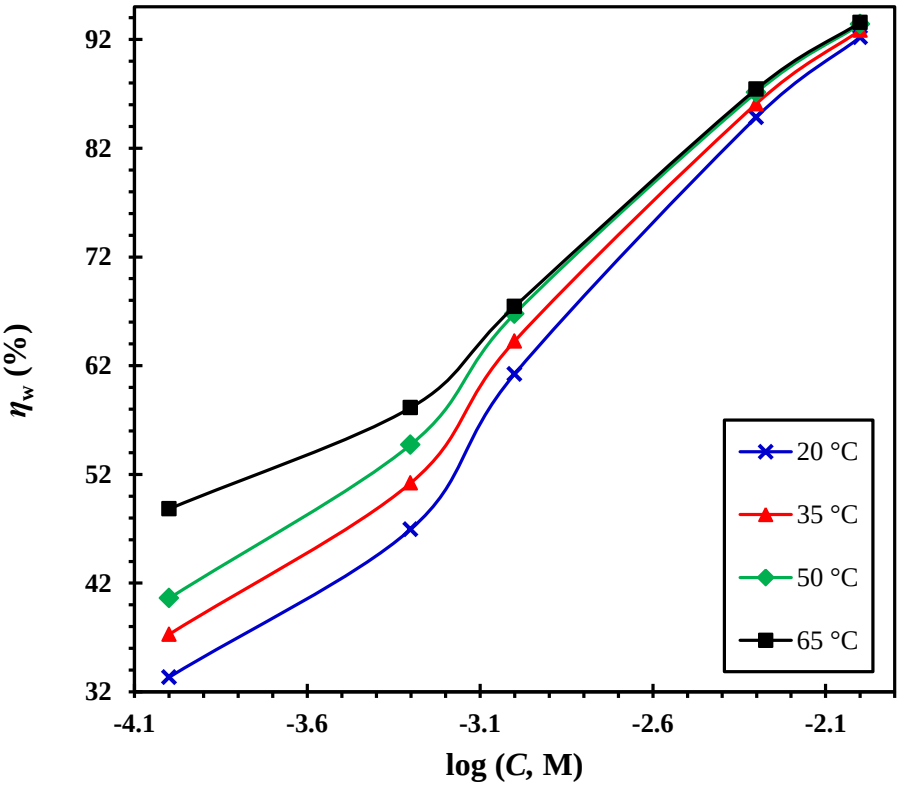

Fig. 4: The variation of inhibition efficiency at different temperatures and different concentrations of the synthesized Schiff base (C).

3. 3. Adsorption behavior and thermodynamic parameters

Corrosion inhibition of metal in acidic media by organic inhibitors is commonly attributed to the adsorption of organic molecules on metal surface, and the inhibition efficiency is directly proportional to surface coverage. The degree of surface coverage (θ) of inhibitor molecules on the carbon steel surface in acidic medium was calculated using the following equation [18, 23, 24].

$$\theta = \frac{W_o - W}{W_o} \qquad (3)$$

where W_o and W are values of the weight loss without and with addition of the inhibitor, respectively.
Trials were carried out to find the isotherm which describes the adsorption mode in the present study. The best fitted isotherm was found to be the Langmuir adsorption isotherm. Langmuir adsorption isotherm postulates the absence of any interaction forces between the adsorbed molecules and the energy of adsorption is independent on the surface coverage value.

Langmuir adsorption isothermal is represented by the following equation [18, 25, 26]:

$$\frac{C}{\theta} = \frac{1}{K_{ads}} + C \qquad (4)$$

where C is the inhibitor concentration, K_{ads} is the adsorptive equilibrium constant.
Fig. 5 shows the relationship between C/θ and C for the prepared Schiff bases at 20, 35, 50 and 65 ºC. From the values of surface coverage, the linear regressions and the slopes of C/θ and C plot were calculated and listed in Table 2. These results show that the linear correlation coefficients (R^2) are almost equal to 1 and all the slopes are very close to 1, which indicated that, the adsorption of inhibitors onto carbon steel surface obeys to the Langmuir adsorption isotherm. Table 2 also reveals that the adsorptive equilibrium constant (K_{ads}) increases with increasing temperature, which indicates that the inhibitor is easily and strongly adsorbed onto the carbon steel surface at relatively higher temperature. This is due to formation of coordinated bond between the prepared Schiff bases and the d-orbital of iron on the surface of steel through the lone pair of electron of N and O atoms.
The equilibrium adsorption constant (K_{ads}) is related to the free energy of adsorption, $\Delta G°_{ads}$ by Eq. (5) [27, 28]:

$$K_{ads} = \frac{1}{55.5}\, exp\left(\frac{\Delta G^o_{ads}}{RT}\right) \qquad (5)$$

where 55.5 is the molar concentration of water in solution expresses in M (mol L^{-1}), R is the gas constant and T is the absolute temperature.

The thermodynamics parameters derived from Langmuir adsorption isotherms for the studied compounds, are given in Table 2. The negative values of ΔG^o_{ads} along with the high K_{ads} indicate a spontaneous adsorption process [29, 30]. Generally, the energy values of -20 kJ mol^{-1} or less negative are associated with an electrostatic interaction between charged molecules and charged metal surface, physisorption. While, those of -40 kJ mol^{-1} or more negative were seen as chemisorption, which is due to the charge sharing or a transfer from the inhibitor molecules to the metal surface to form a covalent bond [31, 32]. The values of ΔG^o_{ads} in our measurements suggested that the adsorption of these Schiff bases involves two types of interaction physisorption and chemisorption.
The adsorption enthalpy can be calculated according to the Van't Hoff equation [33, 34]:

$$\ln K_{ads} = \frac{-\Delta H^o_{ads}}{RT} + \text{constant} \qquad (6)$$

where ΔH^o_{ads} and K_{ads} are the adsorption enthalpy and adsorptive equilibrium constant, respectively. It should be noted that $-\Delta H^o_{ads}/R$ is the slope of the straight line relation between ln K_{ads} and $1/T$ according to Eq. (6). Then the standard adsorption entropy (ΔS^o_{ads}) can be obtained by the basic thermodynamic equation:

$$\Delta G^o_{ads} = \Delta H^o_{ads} - T\Delta S^o_{ads} \qquad (7)$$

The standard adsorption enthalpy (ΔH^o_{ads}) and standard adsorption entropy (ΔS^o_{ads}) were calculated and listed in Table 2. The positive values of ΔH^o_{ads} show that, the adsorption of the inhibitors is an endothermic process, which indicates that, the inhibition efficiency increases with the temperature increasing. Such behavior can be interpreted on the basis that the increase in temperature resulted in sorption of inhibitor molecules on the metal surface [35, 36], ΔS^o_{ads} values in the presence of the inhibitor have positive sign, which mean that, an increase of disorder is due to the adsorption of only one surfactant molecule by desorption of more water molecules [37].

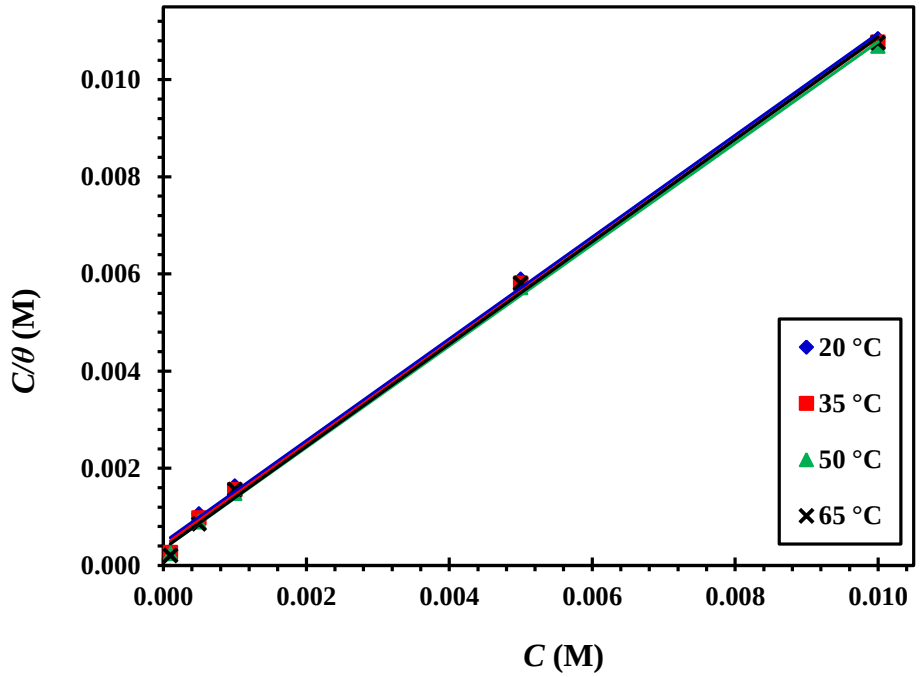

Fig. 5: The Langmuir isotherm adsorption plot for carbon steel in 1 M HCl containing different concentration of the synthesized Schiff base (C) at different temperatures.

Table 2: The thermodynamic parameters of adsorption of the synthesized Schiff bases at different concentrations for carbon steel in 1 M HCl solution

Schiff base	T °C	R^2	slope	K_{ads} M^{-1}	ΔG^o_{ads} kJ mol^{-1}	ΔH^o_{ads} kJ mol^{-1}	ΔS^o_{ads} J mol^{-1} K^{-1}
A	20	0.9982	1.01	1472.8		7.73	
					-27.55		120.43
	35	0.9988	1.02	1828.2			
					-29.52		120.94
	50	0.9990	1.02	2169.2			
					-31.42		121.20
	65	0.9991	1.02	2212.4			
					-32.93		120.30
B	20	0.9940	1.05	880.3	-26.30	11.61	
							129.39
	35	0.9935	1.08	1250.0	-28.55		
							130.38
	50	0.9941	1.08	1543.2	-30.50		
							130.38
	65	0.9942	1.08	1647.5	-32.10		
							129.32
C	20	0.9982	1.04	2141.3		6.09	
					-28.47		117.95
	35	0.9986	1.04	2493.8			
					-30.31		118.20
	50	0.9989	1.04	2924.0			
					-32.22		118.61
	65	0.9983	1.05	2927.6			
					-33.72		117.78

3.4. Potentiodynamic polarization

Both anodic and cathodic polarization curves for carbon steel in 1 M HCl at different concentrations of the prepared Schiff bases at 20 °C are shown in Fig. 6. It is clear that the presence of the inhibitors causes a markedly decrease in the corrosion rate, i.e. shifts the anodic curves to more positive potentials and the cathodic curves to more negative potentials. This may be ascribed to adsorption of the inhibitor over the corroded surface [38]. Values of the corrosion current densities (i_{corr}), corrosion potential (E_{corr}), cathodic Tafel slope (β_c), and anodic Tafel slope (β_a) were obtained from Fig. 6 and listed in Table 3. From these data, it is clear that the corrosion current (i_{corr}) decreases with the increase of the prepared Schiff bases concentration. The presence of the prepared Schiff bases does not remarkably shift the corrosion potential (E_{corr}). Furthermore, anodic and cathodic Tafel constants (β_a and β_c) do not change regularly with increasing concentration of the inhibitor, i.e. Schiff bases affect both the anodic and cathodic overpotentials and shifts Tafel lines parallely in both directions. Therefore, Schiff bases can be classified as mixed-type inhibitors for carbon steel in 1 M HCl. This indicates also that the used inhibitors, at varying concentrations, do not alter the corrosion reaction mechanism. These results suggest that the inhibiting action of such compounds occurs by simple site blocking of the electrode, and thus decrease the surface area available for corrosion reactions [39].
The inhibition efficiency (η_p) is calculated from the following equation:

$$\eta_P = \left(\frac{i_{corr} - i_{corr}(inh)}{i_{corr}}\right) \times 100 \qquad (10)$$

where i_{corr} and i_{corr} (inh) are the corrosion current density values without and with the inhibitor, respectively. The corrosion current density was determined by extrapolation of Tafel lines to the corrosion potential.
Values of the inhibition efficiencies were calculated and listed in Table 3, which reveal that the inhibition efficiency (η_p) increases with increment of the inhibitors concentration. The inhibition efficiency decreases in the following order: C > A > B.

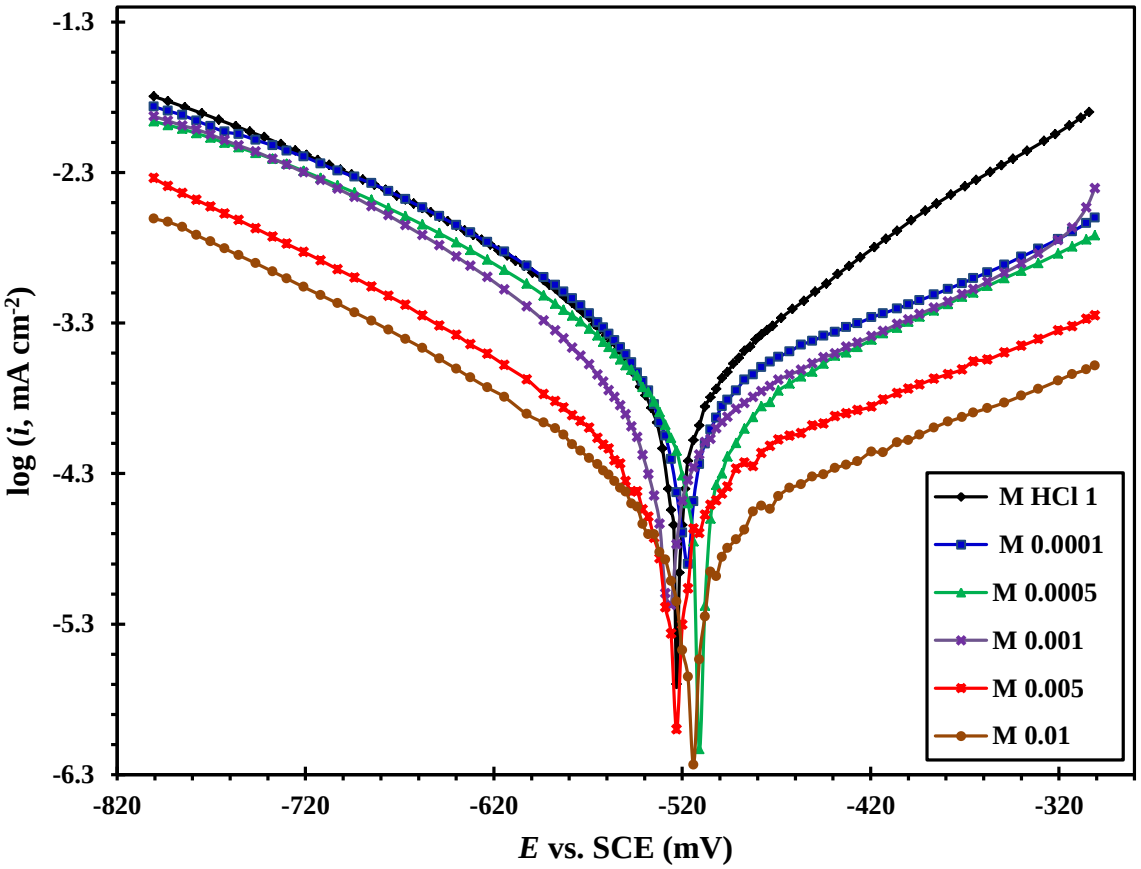

Fig. 6: Anodic and cathodic polarization curves obtained at 20 °C in 1 M HCl with and without different concentration of synthesized Schiff bases (C).

Table 3: Potentiodynamic polarization results for carbon steel in 1 M HCl with and without different concentrations of the synthesized Schiff bases at 20 °C.

Inhibitor	Conc. of inhibitor M	E_{corr} mV	i_{corr} mA cm^{-2}	β_a mV dec^{-1}	β_c mV dec^{-1}	η_p %
1 M HCl	0.00	-524.5	0.5229	164.9	-178.7	-
A	1x10^{-4}	-536.5	0.4546	171.5	-163.9	13.06
	5x10^{-4}	-533.5	0.3578	146.7	-115.6	31.57
	1x10^{-3}	-523	0.1897	139.8	-149.3	63.72
	5x10^{-3}	-535	0.0611	254.6	-119.1	88.32
	1x10^{-2}	-517.3	0.043093	248.2	-248.8	91.76
B	1x10^{-4}	-535	0.48	256.6	-140.3	8.20
	5x10^{-4}	-515	0.38	146.7	-140.3	27.33
	1x10^{-3}	-526.1	0.2759	213.7	-113.4	47.24
	5x10^{-3}	-515.5	0.1496	237.1	-142.5	71.39
	1x10^{-2}	-526.7	0.0652	254.6	-139.8	87.53
C	1x10^{-4}	-518.1	0.3586	289.1	-152.9	31.42
	5x10^{-4}	-511	0.2955	274.2	-111.3	43.49
	1x10^{-3}	-526	0.211	241.1	-136.1	59.65
	5x10^{-3}	-523	0.08	282.3	-154.7	84.70
	1x10^{-2}	-514	0.04136	284.2	-154.7	92.09

3.5. Electrochemical impedance spectroscopy

The corrosion behavior of carbon steel in 1 M HCl solution was investigated in absence and presence of different concentrations of the prepared Schiff bases using electrochemical impedance spectroscopy at 20 °C. Fig. 7 shows that the impedance diagrams, display one single capacitive loop as represented by slightly depressed semi-circle for the studied compound. This capacitive loop indicates that the corrosion of carbon steel in 1 M HCl solution is mainly controlled by the charge transfer process and the formation of a protective layer on the metal surface in the presence of inhibitors. The Phase plots of the carbon steel in 1 M HCl in the absence and presence of the synthesized inhibitors are shown in Fig. 8. It was found that the Phase plots give one time constant only. The charge transfer resistance values (R_{ct}) were calculated from the difference between impedance values at the lower and higher frequencies as suggested by Haruyama et al. [40]. All experimental spectra were fitted with an appropriate equivalent circuit, depicts the proposed equivalent circuit which consists of a solution resistance R_s in series to the constant phase element CPE and the charge transfer resistance R_{ct} while CPE is parallel to R_{ct}. The use of CPE type impedance had been extensively stated by previous reports [41, 42]. The double layer capacitance, C_{dl}, for a circuit including a CPE was calculated from the following equation [43, 44]:

$$C_{dl} = Y_o(\omega_{max})^{n-1} \qquad (11)$$

where $\omega_{max} = 2\pi f_{max}$ and $f_{max}$is the frequency at which the imaginary component of the impedance is maximal. The impedance of CPE is calculated from the following equation [42]:

$$Z_{CPE} = \frac{1}{Y_o(j\omega)^n} \qquad (12)$$

where, Y_o is a proportional factor, $j^2 = -1$, $\omega = 2\pi f$ and n is the phase shift. For $n = 0$, Z_{CPE} represents a resistance with $R = Y_o^{-1}$, for $n = 1$, a capacitance with $C = Y_o$, for $n = 0.5$, a Warburg impedance with $W = Y_o$ and for $n = -1$, an inductive with $L = Y_o^{-1}$.

From data in Table 4, it is clear that n values ranged between 0.73 to 0.90 and this indicating that the electrical double layers are regarded as capacitive double layers.

The inhibition efficiency (η_I) of carbon steel corrosion is calculated from R_{ct} as follows [18]:

$$\eta_I = \frac{R_{ct}(inh) - R_{ct}}{R_{ct}(inh)} \times 100 \qquad (13)$$

where R_{ct} and R_{ct} (inh) are the charge transfer resistance values without and with inhibitor, respectively.
Various impedance parameters and inhibition efficiency (η_I) were calculated and listed in Table 4. As it can be seen from Table 4, the R_{ct} values increase while C_{dl} values decrease with the inhibitor concentration increment. Decrease in the capacitance, which can result from a decrease in local dielectric constant and/or an increase in the thickness of the electrical double layer, suggests that the inhibitor molecules act by adsorption at the metal/solution interface [45]. The addition of the synthesized Schiff bases provides lower C_{dl} values, probably as a consequence of replacement of water molecules by the synthesized inhibitors at the electrode surface. Also the inhibitor molecules may reduce the capacitance by increasing the double layer thickness according to the Helmholtz model [46]: The value of C_{dl} is always smaller in the presence of the inhibitor than in its absence, as a result of the effective adsorption of the synthesized inhibitors.

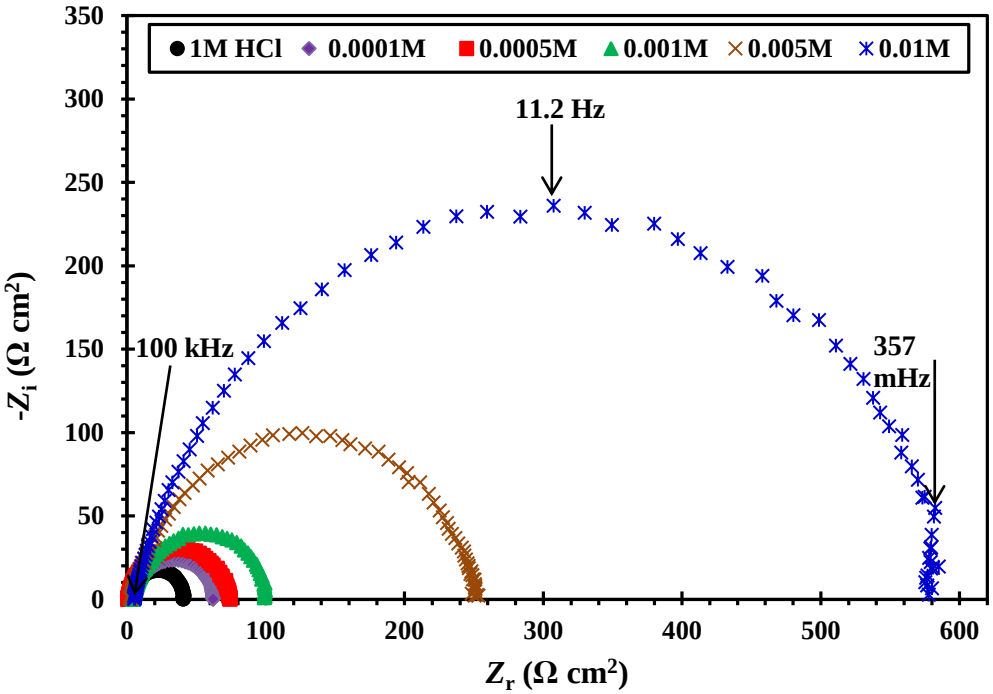

Fig. 7: Nyquist plots for carbon steel in 1 M HCl in absence and presence of different concentrations of Synthesized Schiff base (C) at 20 °C.

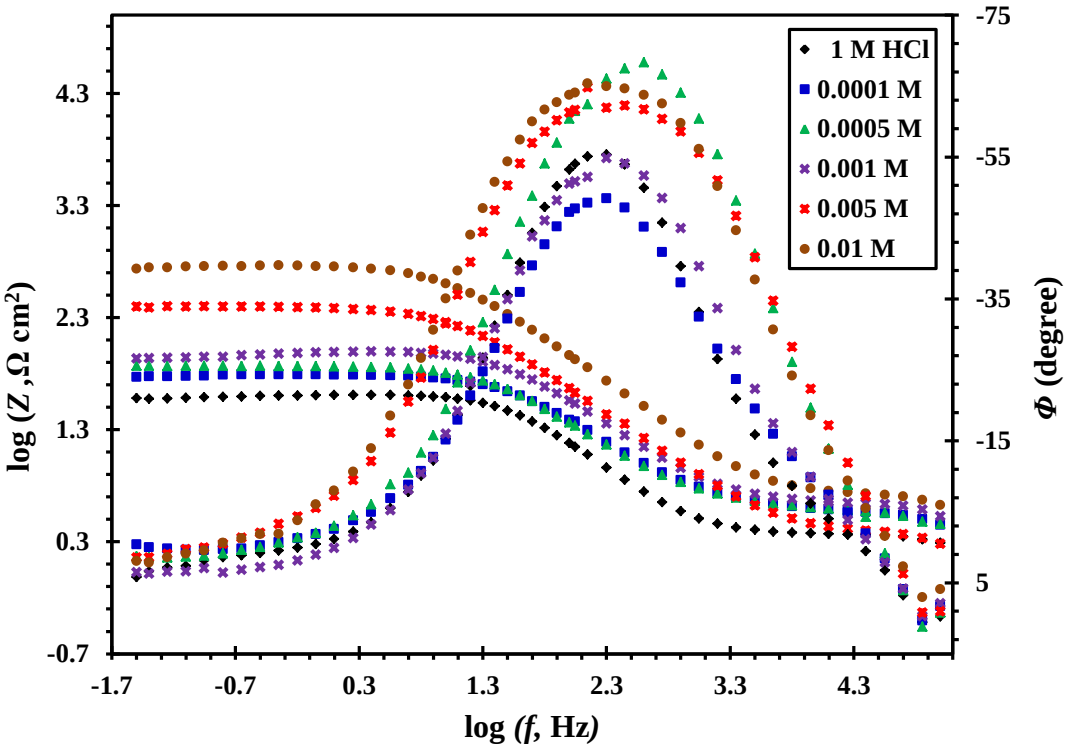

Fig. 8: Bode plot for carbon steel in 1 M HCl in absence and presence of different concentrations of Synthesized Schiff base (C) at 20 °C.

Table 4: Electrochemical impedance parameters for carbon steel in 1 M HCl with and without different concentrations of the synthesized Schiff bases at 20 °C

Schiff base	Conc. of inhibitor M	R_s Ω cm^2	Q_{dl} μΩ^{-1} s^n cm^{-2}	n	Error of n	R_{ct} Ω cm^2	C_{dl} μF cm^{-2}	η_I %
Blank	0.00	2.3	0.1871	0.90	0.79	39.28	136.59	-
A	1x10^{-4}	0.4	0.6303	0.85	0.56	45.66	124.01	13.97
	5x10^{-4}	0.6	0.4105	0.83	0.58	61.21	77.36	35.83
	1x10^{-3}	1.0	0.1347	0.89	0.70	120.0	29.11	67.27
	5x10^{-3}	5.2	0.0501	0.89	0.46	305.3	15.49	87.13
	1x10^{-2}	10.7	0.0401	0.86	0.33	578.7	6.42	93.21
B	1x10^{-4}	0.7	0.3481	0.85	0.60	46.13	117.79	14.85
	5x10^{-4}	0.9	0.1597	0.77	0.51	57.18	88.65	31.30
	1x10^{-3}	0.9	0.1152	0.73	0.62	82.64	49.02	52.47
	5x10^{-3}	5.6	0.0665	0.87	0.91	137.4	20.51	71.41
	1x10^{-2}	3.8	0.0852	0.86	0.42	296.1	16.20	86.73
C	1x10^{-4}	3.9	0.1910	0.82	0.96	59.28	83.61	33.74
	5x10^{-4}	1.0	0.1256	0.90	0.61	72.72	75.59	45.98
	1x10^{-3}	4.3	0.0912	0.87	0.98	97.24	45.19	59.61
	5x10^{-3}	2.3	0.0997	0.83	0.58	252.0	16.78	84.41
	1x10^{-2}	5.1	0.0433	0.85	0.47	579.9	6.70	93.23

3.6. Quantum calculations

Quantum chemical calculations were performed in order to analyze the effect of molecular structure and also electronic parameters on present inhibitor performance [47]. It has been found that the effectiveness of a corrosion inhibitor can be related to its electronic and molecular structure [48-53]. In this study, the relationship between quantum chemical parameters and inhibition efficiency was investigated in Table 5. Frontier molecular orbital density distributions of the synthesized Schiff bases are shown in Fig. 9. Table 5 shows the values of some quantum chemical

parameters, namely the energy of the highest occupied molecular orbital (E_{HOMO}) which is often associated with the capacity of a molecule to donate electron. High value of E_{HOMO} probably indicates a tendency of the molecule to donate electrons to appropriate acceptor molecules with low energy and empty molecular orbital, energy of the lowest unoccupied molecular orbital (E_{LUMO}) indicates the ability of the molecule to accept electrons. The lower value of E_{LUMO}, the more probable is that the molecule would accept electrons [54], According to frontier orbital theory, the reaction of reactants mainly occur on HOMO and LUMO [55]. So, the energy gap is calculated from the following equation:

$$\Delta E = E_{LUMO} - E_{HOMO} \qquad (14)$$

ΔE is the more probable to donate and accept electrons. The values of ΔE in Table 5, suggesting the strongest ability of the synthesized inhibitors to form coordinate bonds with d-orbitals of metal through donating and accepting electrons, is in good agreement with the experimental results and show that Schiff bases are in order C > A > B in inhibition efficiency. Additionally, for the dipole moment (μ), higher value of μ will favor the enhancement of corrosion inhibition [56]. From Table 5, the value of μ is higher, also in agreement with the experimental results mentioned above.
Another method to correlate inhibition efficiency with parameters of molecular structure is to calculate the fraction of electrons transferred from inhibitor to metal surface. According to Koopman's theorem [57], E_{HOMO} and E_{LUMO} of the inhibitor molecule are related to the ionization potential (I) and the electron affinity (A), respectively. The ionization potential (I) and the electron affinity (A) are defined as follows:

$$I = -E_{HOMO} \qquad (15)$$
$$A = -E_{LUMO} \qquad (16)$$

Then absolute electronegativity (X) and global hardness (γ) of the inhibitor molecule are approximated as follows [58]:

$$X = \frac{I + A}{2} \qquad (17)$$
$$\gamma = \frac{I - A}{2} \qquad (18)$$

Thus the fraction of electrons transferred from the inhibitor to metallic surface, ΔN, is calculated by the following equation [49]:

$$\Delta N = \frac{X_{Fe} - X_{inh}}{2(\gamma_{Fe} + \gamma_{inh})} \qquad (19)$$

For calculation of the fraction of electrons transferred, the theoretical values of X_{Fe} (7 eV mol^{-1}) and γ_{Fe} (0 eV mol^{-1}) are used. The calculated results are presented in Table 5. Generally, value of ΔN shows inhibition efficiency resulting from electron donation, and the inhibition efficiency increases with the increase in electron-donating ability to the metal surface. The results indicate that ΔN values correlates strongly with experimental inhibition efficiencies. Thus, the highest fraction of electrons is associated with the best inhibitor (Schiff base C), while the least fraction is associated with the inhibitor that has the least inhibition efficiency (Schiff base B). the inhibition efficiency increases with increasing electron-donating ability at the metal surface. Based on these calculations, it is expected that the synthesized inhibitors are donor of electrons, and the carbon steel surface is the acceptor, and this favors chemical adsorption of the inhibitor on the electrode surface. Here the inhibitor binds to the steel surface and forms an adsorption layer against corrosion. The synthesized inhibitors show the highest inhibition efficiency because it has the highest HOMO energy and this reflects the greatest ability (the lowest ΔE) of offering electrons. It can be seen from Table 3 that the ability of the synthesized inhibitors to donate electrons to the metal surface, which is in good agreement with the higher inhibition efficiency of the synthesized inhibitor. Another evidence show that the synthesized Schiff bases are efficient inhibitors is the hardness (γ) which can be calculated from the following equation:

$$\gamma = \frac{I - A}{2} \qquad (18)$$

and softness from the following equation [58]:

$$\delta = \frac{1}{\gamma} \qquad (20)$$

It is evident that the inhibitor with the least value of global hardness (hence the highest value of global softness) is the best. This is because a soft molecule is more reactive than a hard molecule. This observation is consistent with the results obtained from experimental inhibition efficiencies.

HOMO LUMO

Schiff base (A)

HOMO LUMO

Schiff base (B)

HOMO LUMO

Schiff base (C)

Fig. 9: Frontier molecular orbital density distributions of the synthesized Schiff bases.

Table 5: The structure parameters and adsorptive performance of the synthesized Schiff bases

Schiff base	E_H eV	E_L eV	ΔE eV	X eV	γ eV	δ eV^{-1}	μ D	π eV	M_g $cm^3\ mol^{-1}$	ΔN e	Total energy a.u.
A	-8.195	-0.413	7.782	4.304	3.891	0.257	3.07	-4.304	165.786	0.346	-615.77
B	-8.232	-0.398	7.834	4.315	3.917	0.255	2.38	-4.315	107.258	0.343	-459.92
C	-5.325	-0.674	4.651	2.999	2.326	0.430	4.23	-2.999	163.016	0.860	-612.36

3.7. Inhibition mechanism

The adsorption of organic molecules on the solid surfaces cannot be considered only as purely physical or as purely chemical adsorption phenomenon. In physical adsorption, the inhibitor molecules can be adsorbed on the steel surface via electrostatic interaction between the charged metal surface and charged inhibitor molecule. While in the chemical adsorption of the studied Schiff bases arises from the donor acceptor interactions between free electron pairs of the hetero atoms and p electrons of multiple bonds as well as phenyl group and vacant d-orbitals of iron [59, 60]. It has been reported that the adsorption of heterocyclic compounds occurs with the aromatic rings sometimes parallel but mostly normal to the metal surface. The orientation of molecules could be dependent on the pH and/or electrode potential. However, more work should be provided to confirm the above arguments [61]. In the case of parallel adsorption of inhibitor molecules, the steric factors also must be taken into consideration The adsorption free energy values are ranged between -20 and -40 kJ mol^{-1} which indicate that the adsorption mechanism of the tested Schiff bases on carbon steel surface in 1 M HCl solution is a mixed of physical and chemical adsorption. Schiff bases have basic character and expected to be protonated in equilibrium with the corresponding neutral form in strong acid solutions. It is also well known that steel surface in 1 M HCl charges negative charge because of E_{corr} - $E_{q=0}$ (zerochargepotential) < 0, thus, it is easily for the positively charged inhibitors to approach the negatively charged steel surface due to the electrostatic attraction. At high temperatures, the donor acceptor interaction between free electron pairs of nitrogen atom, oxygen atom and phenyl ring of the synthesized inhibitors and vacant d-orbital's of iron was found. The adsorption of Schiff bases molecules reduced the rate of hydrogen evolution reaction. It was found that the best Schiff base was Schiff base (C). This could be due to phenol group (more activating) in inhibitor (C), which can form coordinated bonds with the carbon steel due to high electron density on phenyl group and tow lone pairs of electron on (OH) group in addition to the hydrophobicity and planarity of benzene ring on the steel surface. Schiff base (A) that contain phenyl ethyl group is weaker electron donors than a phenol group because ethyl group (CH_2CH_2) not electron donor group that showed a lower inhibition efficiency than Schiff base (C). While Schiff base (B) containing ethanol group show the least inhibition efficiency because (OH) group is less than phenyl group in electron donation.

The studied Schiff bases showed more enhanced inhibition efficiency values (87-92%, at 0.01M) than the reported ones. Bouklah et al [62] proposed that the effect of synthesized diethyl 2-(2-oxopyrrolidin-1-yl) ethyl phosphonate (P1) on the corrosion of steel in 0.5 M H_2SO_4 solution has been studied. The inhibition efficiency increases with the concentration of P1 to attain 86% at $5x10^{-3}$ M. Bouklah et al [63] reported the corrosion inhibition by 1-{2-[(2 hydroxyethyl)thio]ethyl}pyrrolidin-2-one (HTEP) and {[2-(2-oxopyrrolidin-1-yl)ethyl]thio}acetic acid (OETA) as corrosion inhibitors for steel in 0.5 M H_2SO_4. The inhibition efficiencies at $5x10^{-3}$ are 89 and 86 respectively.

4. Conclusions

1. The chemical structures of the synthesized Schiff bases are confirmed by ^{1}HNMR and Mass spectroscopy.
2. The inhibition efficiency of the synthesized Schiff bases increases with increasing the concentration and increases with increasing temperature in range 20- 65 °C.
3. The adsorption of the synthesized Schiff bases on the carbon steel surface is physical adsorption and chemical adsorption and obeyed Langmuir isotherm.
4. Tafel polarization curves indicate that the corrosion current density decreases and the corrosion potential changes with the addition of the Schiff bases, therefore the synthesized Schiff bases are a mixed types.
5. Double-layer capacitances decrease with respect to blank solution when the synthesized inhibitor is added. This fact can be explained by adsorption of the synthesized inhibitor species on the steel surface.
6. The smaller gap between E_{HOMO} and E_{LUMO} favors the adsorption of the synthesized Schiff bases on iron surface and enhancement of corrosion inhibition.

References

[1] G.L. Higgins, R.S. Hullcoop, S. Turgoose, W. Bullough, Corrosion (2010) 2483–2493.
[2] P.B. Raja, A.K. Qureshi, A.A. Rahim, H. Osman, K. Awang, Corros. Sci. 69 (2013) 292‑301.
[3] R. Solmaz, Corros.Sci. 79 (2014) 169‑176.
[4] M. Tourabi, K. Nohair, M. Traisnel, C. Jama, F. Bentiss, Corros Sci. 75 (2013) 123‑133
[5] M.J. Bahrami, S.M.A. Hosseinia, P. Pilvar, Corros. Sci. 52 (2010) 2793‑2803.
[6] L. Fragoza-Mar, O. Olivares-Xometl, M.A. Dominguez-Aguilar, E.A. Flores, P. Arellanes-Lozada, F. Jimenez-Cruz, Corros. Sci. 61 (2012) 171‑184.
[7] M.M. Solomon, S.A. Umoren, I.I. Udosoro, A.P. Udoh, Corros. Sci. 52 (2010) 1317‑1325.
[8] B. Obat, N.O. Obi-Egbedi, Corros. Sci. 52 (2010) 198–204.
[9] Y. G. Avdeev, Y. I. Kuznetsov, A. K. Buryak, Corros. Sci. 69 (2013) 50‑60.
[10] M. Bouklah, B. Hammouti, M. Lagrenee, F. Bentiss, Corros. Sci. 48 (2006) 2831–2842.

[11] S. Deng, X. Li, X. Xie, Corros. Sci. 80 (2014) 276‑289.
[12] A. Adewuyia, A. Göpfertb, T. Wolff, Industrial Crops and Products 52 (2014) 439– 449.
[13] B. O. Hasan, S. A. Sadek, Eng. Chem. 20 (2014) 297–307.
[14] M.N. Katariya, A.K. Jana, P.A. Parikh, Industrial and Eng. Chem. 19 (2013) 286.
[15] C. M. Goulart, A. Esteves-Souza, C. A. Martinez-Huitle, C. J. F. Rodrigues, M. Aparecida M. Maciel, A. Echevarria, Corros. Sci. 67 (2013) 281‑291.
[16] F.S. de Souza, A. Spinelli, Corros. Sci. 51 (2009) 642‑649.
[17] M. Lebrini, F. Bentiss, H. Vezin, M. Lagrenée, Corros. Sci. 48 (2006) 1279–1291.
[18] M.A. Hegazy, A.M. Badawi, S.S. Abd El Rehim, W.M. Kamel, Corros. Sci. 69 (2013) 110‑122.
[19] M.W. Schmidt, K.K. Baldridge, J.A. Boatz, S.T. Elbert, M.S. Gordon, J.H. Jensen, S.Koseki, N. Matsunaga, K.A. Nguyen, S.J. Su, T.L. Windus, M. Dupuis, J.A.Montgomery, J.Comput. Chem. 14 (1993) 1347–1363.
[20] M.A. Hegazy, M. Abdallah, M.K. Awad d, M. Rezk, Corros. Sci. (2014) 54‑64.
[21] Z. Tao, S. Zhang, W. Li, B. Hou, Corros. Sci. 51 (2009) 2588–2595.
[22] K.F. Khaled, M.A. Amin, Corros. Sci. 51 (2009) 1964–1975.
[23] V.V. Torres, V.A. Rayol, M. Magalhaes, G.M. Viana, L.C.S. Aguiar, S.P. Machado, H. Orofino, E. D' Elia, Corros. Sci. 79 (2014) 108‑118.
[24] I. Ahamad, M.A. Quraishi, Corros. Sci. 51 (2009) 2006–2013.
[25] V.V. Torres, R.S. Amado, C.F. de Sa, T.L. Femandez, C.A. Da Silva Riehl, A.G. Torres, E. D' Elia, Corros. Sci. 53 (2011) 2385‑2392.
[26] M.A. Hegazy, M.F. Zaky, Corros. Sci. 52 (2010) 1333–1341.
[27] D. Daoud, T. Douadi, S. Issaadi, S. Chafaa, Corros. Sci. 79 (2014) 50–58.
[28] G. Mu, X. Li, Q. Qu, J. Zhou, Corros. Sci. 48 (2006) 445.
[29] F. Bentiss, M. Lebrini, M. Lagrene, Corros. Sci. 47 (2005) 2915–2931.
[30] Z. Szklarska-Smialowska, J. Mankowski, Corros. Sci. 18 (1978) 953–960.
[31] A. Khamis, M.M. Saleh, M.I. Awad, B.E. El-Anadouti, Corros. Sci. 74 (2013) 83‑91.
[32] Q. Qu, Z. Hao, L. Li, W. Bai, Z. Ding, Corros. Sci. 51 (2009) 569.
[33] M.A. Hegazy, A.S. El-Tabei, A.H. Bedair, M.A. Sadeq, Corros. Sci. 41 54 (2012) 219‑230.
[34] G. Quartarone, M. Battilana, L. Bonaldo, T. Tortato, Corros. Sci. 50 (2008) 3467.
[35] C.M. Goulart, A. Esteves-Souza, C.A. Martinez-Huitle, C.J.F. Rodrigues, M.A.M. Maciel, A. Echevarria, Corros. Sci. 67 (2013) 281‑291.
[36] M. Behpour, S.M. Ghoreishi, N. Soltani, M. Salavati-Niasari, M. Hamadanian, A. Gandomi, Corros. Sci. 50 (2008) 2172–2181.
[37] M. Abdallah, Corros. Sci. 44 (2002) 717– 728.
[38] R.A. Prabhu, T.V. Venkatesha, A.V. Shanbhag, G.M. Kulkarni, R.G. Kalkhambkar,Corros. Sci. 50 (2008) 3356.
[39] A. Doner, E.A. Sahin, G. Kardas, O. Serindag, Corros. Sci. 66 (2013) 278‑284.
[40] S. Haruyama, T. Tsuru, B. Gijutsu, J. Jpn. Soc. Corros. Engg. 27 (1978) 573.
[41] A. Popova, M. Christov, Corros. Sci. 48 (2006) 3208–3221.
[42] K.S. Jacob, G. Parameswaran, Corros. Sci. 52 (2010)224–228.
[43] C.H. Hsu, F. Mansfeld, Corrosion 57 (2001) 747‑748.
[44] A. Popova, M. Christov, A. Vasilev, Corros. Sci. 53 (2011) 1770–1777.
[45] Y. Tang, X. Yang, W. Yang, Y. Chen, R. Wan, Corros. Sci. 52 (2010) 242‑249.
[46] E.E. Oguzie, Y. Li, F.H. Wang, Electrochim. Acta 53 (2007) 909.
[47] A. Kosari, M.H. Moayed, A. Davoodi, R. Parvizi, M. Momeni, H. Eshghi, H. Moradi, Corros. Sci. 78 (2014) 138-150.
[48] E. E. Ebenso, D. A. Isabirye, N. O. Eddy, Int. J. Mol. Sci. 11 (2010) 2473-2498.
[49] E. E. Ebenso, M. M. Kabanda1, T. Arslan, M. Saracoglu, F. Kandemirli, L. C. Murulana, A. K. Singh, S. K. Shukla, B. Hammouti, K.F. Khaled, M.A. Quraishi, I.B. Obot, N.O. Eddy, Int. J. Electrochem. Sci., 7 (2012) 5643 – 5676.
[50] S. Xia, M. Qiu, L. Yu, F. Liu, H. Zhao, Corros. Sci. 50 (2008) 2021-2029.
[51] E.E. Ebenso, T. Arslan, F. Kandemirli, N. Caner, I. Love, Int. J. Quantum Chem. 110 (2010) 1003-1018.
[52] T. Arslan, F. Kandemirli, E.E. Ebenso,I. Love, H. Alemu, Corros. Sci. 51(2009) 35-47.
[53] I.B. Obot, N.O. Obi-Egbedi, Corros. Sci. 52 (2010) 657.
[54] Z. El Adnani, M. Mcharfi, M. Sfaira, M. Benzakour, Corros. Sci. 68 (2013) 223-230.
[55] N. Khalil, Electrochim. Acta 48 (2003) 2635–2640.
[56] J. Zhang, J. Liu, W. Yu, Y. Yan, L. You, L. Liu, Corros. Sci. 52 (2010) 2059–2065.
[57] M. Lebrini, M. Lagrenee, M. Traisnel, L. Gengembre, H. Vezin, F. Bentiss, Appl. Surf. Sci. 253 (2007) 9267–9276.

[58] T.P. Trainor, A.M. Chaka, P.J. Eng, M. Newville, G.A. Waychunas, J.G. Catalano, G.E. Brown, Jr. Surf. Sci. 573(2004) 204-224.
[59] M. Behpour, S.M. Ghoreishi, M. Salavati-Niasari, B. Ebrahimi, Mater. Chem. Phys. 107 (2008) 153–157.
[60] A. Yurt, A. Balaban, S. Ustun Kandemir, G. Bereket, B. Erk, Mater. Chem. Phys. 85 (2004) 420–426.
[61] Lj. Vracar, D.M. Drazic, Corros. Sci. 44 (2002) 1669–1680.
[62] M. Bouklah, O. Krim, M. Messali, B. Hammouti, A. Elidrissi; Der Pharma Chemica, 3 (5) (2011) 283-293.
[63] M. Bouklah , H. Harek , R. Touzani, B. Hammouti, Y. Harek; Arabian Journal of Chemistry 5 (2012) 163–166.